Impact of Virtual and Augmented Reality Based on Intraoperative Magnetic Resonance Imaging and Functional Neuronavigation in Glioma Surgery Involving Eloquent Areas

Guo-chen Sun, Fei Wang, Xiao-lei Chen, Xin-guang Yu, Xiao-dong Ma, Ding-biao Zhou, Ru-yuan Zhu, Bai-nan Xu

■ BACKGROUND: **The utility of virtual and augmented reality based on functional neuronavigation and intraoperative magnetic resonance imaging (MRI) for glioma surgery has not been previously investigated.**

■ METHODS: **The study population consisted of 79 glioma patients and 55 control subjects. Preoperatively, the lesion and related eloquent structures were visualized by diffusion tensor tractography and blood oxygen level–dependent functional MRI. Intraoperatively, microscope-based functional neuronavigation was used to integrate the reconstructed eloquent structure and the real head and brain, which enabled safe resection of the lesion. Intraoperative MRI was used to verify brain shift during the surgical process and provided quality control during surgery. The control group underwent surgery guided by anatomic neuronavigation.**

■ RESULTS: **Virtual and augmented reality protocols based on functional neuronavigation and intraoperative MRI provided useful information for performing tailored and optimized surgery. Complete resection was achieved in 55 of 79 (69.6%) glioma patients and 20 of 55 (36.4%) control subjects, with average resection rates of 95.2% ± 8.5% and 84.9% ± 15.7%, respectively. Both the complete resection rate and average extent of resection differed significantly between the 2 groups ($P < 0.01$). Postoperatively, the rate of preservation of neural functions (motor, visual field, and language) was lower in controls than in glioma patients at 2 weeks and 3 months ($P < 0.01$).**

■ CONCLUSION: **Combining virtual and augmented reality based on functional neuronavigation and intraoperative MRI can facilitate resection of gliomas involving eloquent areas.**

INTRODUCTION

Virtual reality (VR) can simulate the real world and provide information that may not be otherwise visible to the naked eye, allowing users to visualize objects within a 3-dimensional (3D) space without limits. However, the lack of interaction between VR and the real world limits its widespread application.[1,2]

Augmented reality (AR) is a new cross-discipline based on VR that superimposes computer-generated virtual objects in real time and space with auxiliary enhancement such that the user perceives a real-world scene rather than a virtual phenomenon (the so-called enhanced concept). AR technology has been preliminarily applied to neurosurgery.[3,4] In this study, we investigated the utility of combined VR and AR for intraoperative magnetic resonance imaging (iMRI) and neuronavigation in glioma surgery.

METHODS

Patient Population

A total of 134 consecutive patients with gliomas involving eloquent (motor, language, and vision) areas were prospectively recruited between February 2009 and January 2014. Of these patients, 79 underwent surgery using functional neuronavigation and iMRI and

Key words
- Augmented reality
- Diffusion tensor imaging
- Functional neuronavigation
- Intraoperative MRI
- Virtual reality

Abbreviations and Acronyms
AQ: Aphasia quotient
AR: Augmented reality
DTT: Diffusion tensor tractography
HGG: High-grade glioma
LGG: Low-grade glioma
VR: Virtual reality

Department of Neurosurgery, PLA General Hospital, Beijing, China

To whom correspondence should be addressed: Xin-guang Yu, M.D., Ph.D. [E-mail: sjwk301@yeah.net]

Citation: World Neurosurg. (2016) 96:375-382.
http://dx.doi.org/10.1016/j.wneu.2016.07.107

Journal homepage: www.WORLDNEUROSURGERY.org

Available online: www.sciencedirect.com

55 underwent surgery guided by anatomic neuronavigation, comprising the patient and control groups, respectively. The study protocol was approved by our institutional ethics committee, and all patients or their family members provided written, informed consent for their participation.

Image Acquisition

Both anatomic MRI, diffusion tensor imaging (DTI), and functional (f)MRI were carried out on a 1.5T scanner (Siemens Espree, Erlangen, Germany) following a standard protocol, as described in our previous study.[5,6]

VR: 3D-Visualized Functional Structures

Lesion Segmentation. The object-creation module of iPlan 2.6 (BrainLab, Feldkirchen, Germany) was used for tumor segmentation. Tumor volumes for high- and low-grade glioma (HGG and LGG, respectively) were calculated automatically by the software on the basis of postcontrast T1/T2 and T2 fluid-attenuated inversion recovery images, respectively. The minimum distance between eloquent areas and the lesion was measured with the object-manipulation function of iPlan 2.6. Patients with a minimum tumor distance <20 mm to any of the eloquent areas were enrolled in the study.

Fiber Tracking and Functional Cortex Localization. The fiber tracking module of the neuronavigation planning software iPlan 3.0 (BrainLab) was used to reconstruct the pyramidal tract, arcuate fasciculus, and optic radiation. The blood oxygen level—dependent mapping module was used for eloquent cortex localization. Broca's and Wernicke's areas and hand, foot, and visual cortices were localized. Details on this procedure are reported elsewhere.[5-7]

Surgical Planning

Surgical planning was optimized by the corresponding author according to the relationship between the 3D-visualized tumor and functional structures (Figure 1).

AR: Microscope-Based Neuronavigation

Integration of 3D-Visualized Functional Structures and Real Skull and Brain. After registering the microscope, the object-visible options were activated. This allowed reconstructed structures of interest to be made visible or invisible at the neurosurgeon's discretion and to be superimposed on the real head through the eyepiece of the registered microscope. Using microscope-based functional neuronavigation, a reasonable incision line was delineated. Additionally, bone flap, extent of cortical incision, and white matter trajectory were determined on the basis of the reconstructed structures visualized through the microscope eyepiece.

Intraoperative Image-Guided Surgical Resection

Virtual images (i.e., reconstructed eloquent structures) can be visualized as a 3D volume or as 2D sections, with the structures represented by different colors. In the 3D volume scene, different levels of transparency provide a sense of depth above and below the focal plane in virtual images. In the 2D image scene, reconstructed structures in the focal plane are delineated with solid lines, while deeper structures are delineated with dotted lines that are omitted in deeper planes. The information gained allows the neurosurgeon to determine the site of surgical manipulation and assess whether or not it was safe.

iMRI of Brain Shift

Residual Tumor and Fiber Tract. Intraoperative imaging provides the possibility of rectifying brain shift and evaluating the extent of tumor resection. If a resectable residual tumor is found, the navigation is updated so that the neurosurgeon can remove the lesion. The fiber tract can also be updated by intraoperative DTI (see Figure 1). For all patients in the present study, MRI was performed within 48 hours of surgery to assess residual tumor volume using iPlan 2.6, as previously described.[5,6]

Intraoperative Functional Cortex Positioning. After opening the dura but before brain shift occurred, cortical function was evaluated by microscope-based functional neuronavigation. Sterile vitamin E capsules were affixed on the cortex using fibrin glue according to the outline of the reconstructed eloquent cortex projected onto the real brain for precise intraoperative positioning of the functional cortex (Figure 2).

Muscle Strength, Aphasia Quotient, and Visual Field Examination

All patients preoperatively underwent muscle strength, aphsia quotient (AQ), and visual field examinations 2 weeks and 3 months after surgery. AQ was obtained by Western Aphasia Battery testing; values $\geq$ 93.8 and $<$ 93.8 were defined as normal and aphasia, respectively. Visual field testing was performed with a Humphrey Field Analyser II (Medtec, Tokyo, Japan) by an experienced ophthalmologist who was blinded to the neuroimaging findings.

Statistical Analysis

The Student's t and χ^2 tests were used to compare initial baseline balance between groups, and the Mann-Whitney U and t tests were used to compare the extent of resection and AQ between the groups. The Mann-Whitney U test was also used to compare muscle strength and visual field scores between the groups, and the paired t test was used to compare initial and final extent of tumor resection in the patient group. A P value < 0.05 was considered statistically significant. Data were analyzed using SPSS v.16.0 software (SPSS Inc., Chicago, Illinois, USA).

RESULTS

General

Glioma patients were diagnosed as LGG [World Health Organization (WHO) grades I and II) or HGG (WHO grades III and IV). The related eloquent area was reconstructed and localized, and their relationship to lesions was demonstrated and recorded in each patient. We defined reconstructed structures related to language (Broca's and Wernicke's areas and arcuate fasciculus), motor (hand and foot cortices and pyramidal tract), and vision (optic radiation and visual cortex) as eloquent areas. Lesion-to-eloquent area distances <20 mm were considered to indicate related functional structures. Details of the analysis are shown in Table 1.

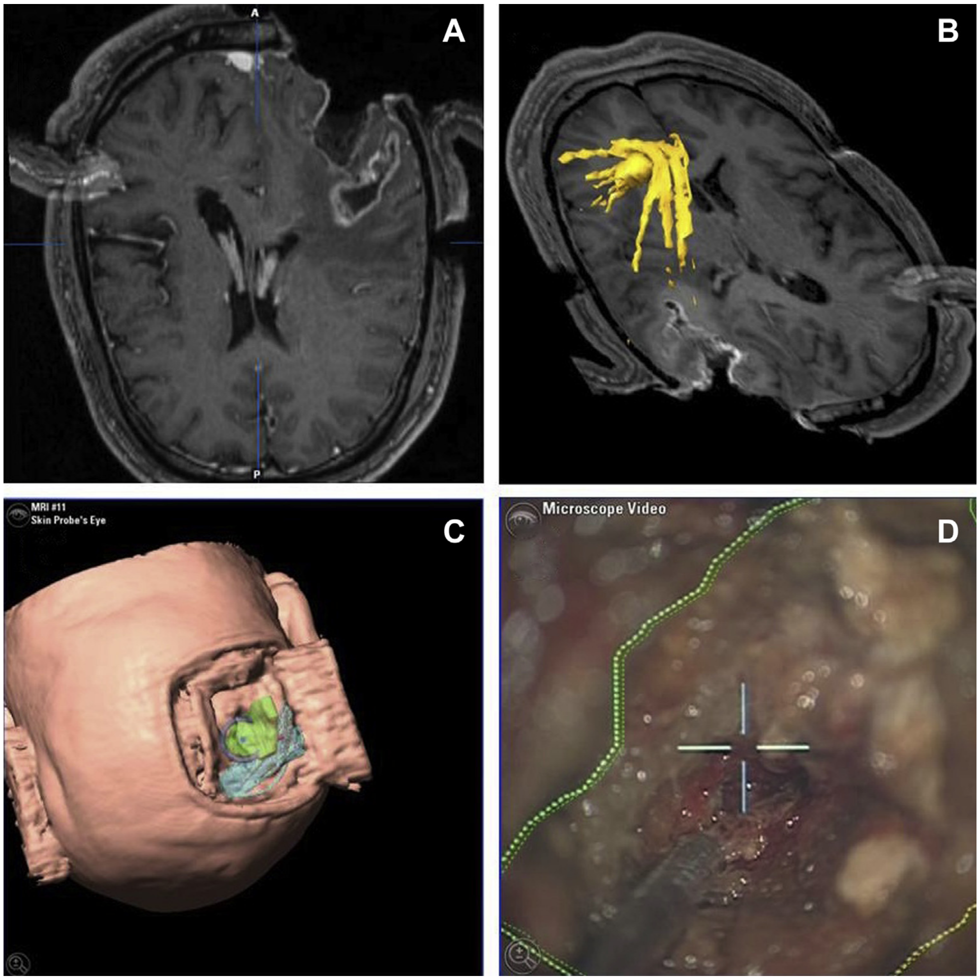

Figure 1. High-grade glioma located in the left temporoparietal lobe. (**A**) Unexpected residual lesions were detected by intraoperative magnetic resonance imaging. (**B**, **C**) Using the virtual reality technique, the residual tumor was outlined and the shifted arcuate fasciculus was reconstructed. (**D**) Augmented reality enables the surgeon to remove the residual tumor by microscope-based functional neuronavigation. The whole process can be repeated until the surgeon is satisfied that all traces of the tumor have been removed.

VR: Surgical Planning Based on Visualized Eloquent Structures. Surgical planning was carried out according to the observed relationship between the lesion and reconstructed eloquent structures, and an optimized surgical approach—including cortical incision and white matter trajectory—was designed (Figure 3). In 17 cases, the surgical approach, including resection site in the cortex or white matter trajectory, was changed on the basis of reconstructed eloquent structures; none of these cases exhibited permanent neurologic deficits.

AR: Intraoperative Tumor and Eloquent Area Visualization-Based Guided Resection and iMRI of Brain Shift

Extent of Resection. iMRI was performed at least once in each patient. In the 79 glioma patients, the first intraoperative imaging series revealed incomplete tumor resection in 39 patients (49.4%), while gross total tumor resection (≥95%) was performed in 40 patients (50.6%). The average residual tumor volumes for LGG and HGG were 6.7 ± 8.4 and 8.1 ± 12.7 cm^3, respectively. Of the 39 glioma patients with residual tumor after the first iMRI, 33 (17 LGG and 16 HGG) underwent further resection. Final intraoperative imaging revealed that 55 of the 79 patients (69.6%) achieved complete resection, with an average extent of resection [(postoperative tumor volume−preoperative tumor volume)/preoperative tumor volume] of 95.2% ± 8.5%. In the control group, final imaging revealed that 20 of the 55 patients (36.4%) achieved complete resection, with an average resection rate of 84.9% ± 15.7%. Both values differed significantly between the 2 groups ($P < 0.01$). Residual volume was decreased from

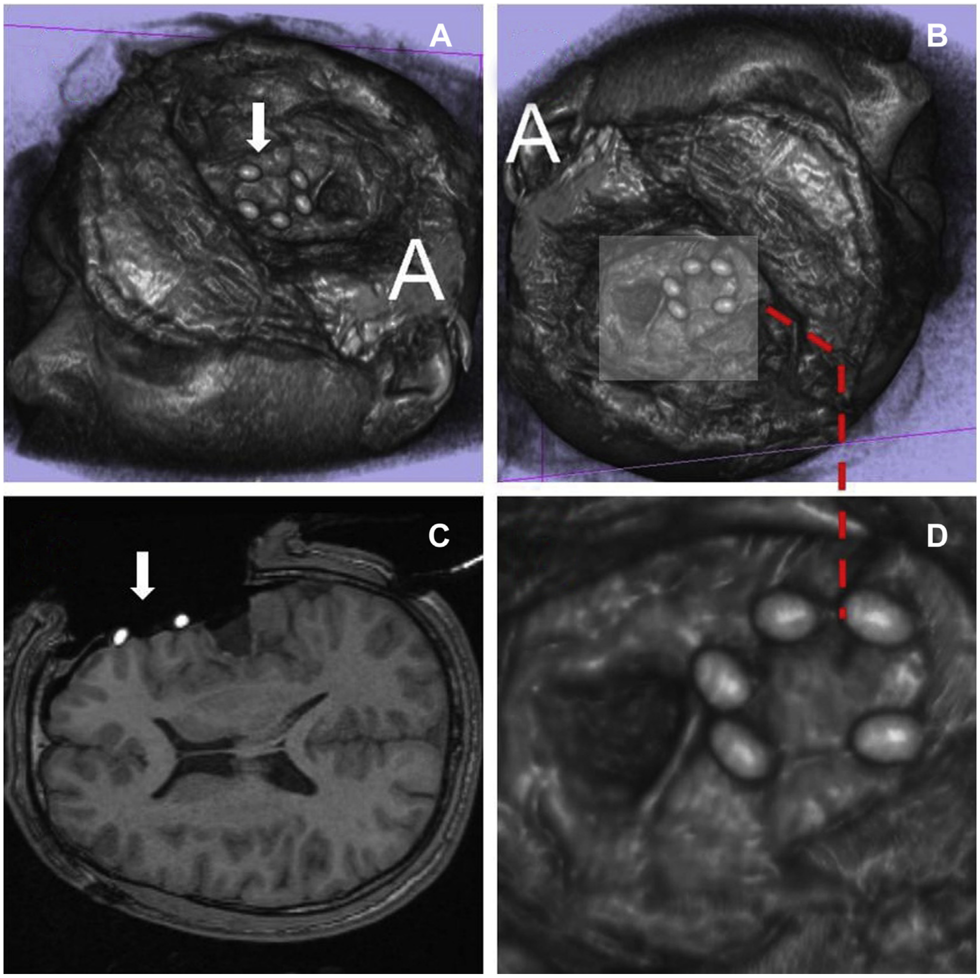

Figure 2. (**A–D**) For intraoperative eloquent cortex localization and preservation, the dura was exposed and vitamin E capsules were used to mark the functional area of the cortex (e.g., Broca area) before brain shift occurred so that no damage occurred. Vitamin E capsules exhibited an intense T1 signal.

7.4 ± 10.7 to 3.2 ± 6.4 cm^3 ($P < 0.01$) with further resection. Details of the extent of resection are shown in Table 2.

Preservation of Neurologic Function. There were no differences in preoperative motor (mean rank: 67.6 vs. 67.4; $P = 0.980$), visual field (mean rank: 67.7 vs. 67; $P = 0.851$), and language (92.1 ± 12.5 vs. 91.3 ± 11.1; $P = 0.688$) functions (constituent ratio and baseline of neuro-functional defects) between glioma patients and controls. Postoperatively, the rates of preservation of all 3 neurologic functions were lower in the control than in the study group at 2 weeks and 3 months ($P < 0.05$). Details of neurofunctional preservation are shown in Table 3.

DISCUSSION

In the study, we found that VR based on functional neuronavigation was useful for optimizing surgical planning. Intraoperative 3D visualization of lesions and their associated functional structures (AR) can provide information to neurosurgeons for performing specific manipulations. Moreover, iMRI can detect brain shift during the surgical process and provide quality control during surgery. Most previous studies have focused on a single type of neurologic function, and the relationship between the eloquent area and the extent of resection has never been examined. In the present study, we investigated all of the associated eloquent areas, which more accurately reflects reality. Our findings revealed that combining the previously described techniques significantly improved tumor resection rate and neurofunctional preservation.

Help of VR

Surgical planning using anatomic neuronavigation is based on skull anatomy and brain structures. Brain anatomic labels vary

Table 1. Statistical Analysis of Initial Baseline Between 2 Groups

	Study Group	Control Group	Statistical Analyses and *P* Value
Age (years)	40.9 ± 14.7	45.2 ± 15.7	$t = -1.636$, $P = 0.104$
Gender (male/total)	54/79	40/55	$X^2 = 0.296$, $P = 0.586$
Preop. tumor volume (cm^3)	53.1 ± 24.3	49.9 ± 23.8	$t = 0.749$, $P = 0.455$
Tumor grade (LGG/total)	39/79	29/55	$X^2 = 0.146$, $P = 0.702$
Muscle strength			
Related cases	47/79	26/55	$X^2 = 1.953$, $P = 0.162$
Mean distance (mm)	4.3 ± 4.8	3.2 ± 4.0	$t = 1.006$, $P = 0.318$
Language			
Related cases	42/79	31/55	$X^2 = 0.134$, $P = 0.715$
Mean distance (mm)	4.5 ± 4.8	3.2 ± 5.1	$t = 1.106$, $P = 0.272$
Visual field			
Related cases	48/79	37/55	$X^2 = 0.593$, $P = 0.441$
Mean distance (mm)	3.4 ± 4.1	3.8 ± 4.3	$t = -0.422$, $P = 0.674$
Preop. AQ	92.11 ± 12.47	91.27 ± 11.07	$t = 0.402$, $P = 0.688$
Preop. muscle strength (0—5)*	4.6 ± 0.5	4.6 ± 0.6	$Z = -0.025$, $P = 0.980$
Preop. vision defect (0—2)†	0.3 ± 0.5	0.2 ± 0.5	$Z = -0.187$, $P = 0.851$

*Muscle strength was evaluated by muscle strength grading scale (Oxford scale).
†0, normal visual field; 1, quadrantanopia; 2, hemianopsia.

considerably; as such, anatomic markers for lesion sites are often unreliable. Additionally, brain structures cannot be visually distinguished by the neurosurgeon,[8,9] making it difficult to optimize surgical planning without an evidence-based surgical planning system. Moreover, different surgeons can have distinct perspectives on the same patient even when guided by anatomic neuronavigation. There are currently several surgical planning systems based on skull and brain anatomy that do not provide accurate localization of structures.[10-12]

Using the surgical planning system based on VR technology, cortical positions and fiber tracts were defined by fMRI and tractography, respectively, so as to visualize related preoperative 3D structures. This enabled the neurosurgeon to determine the position of lesions in relation to these structures from any angle, which revolutionizes neurosurgical planning.

Importance of AR

In control patients, functional preservation and extensive lesion removal are difficult to achieve in the absence of visible structures. Thus the neurosurgeon may destroy surrounding normal tissue to avoid leaving residual tumor cells, or else carry out incomplete resection in an attempt to preserve neurologic function.

Intraoperative AR, which enables visualization of lesions and structures, can resolve this issue[13,14] because the surgeon can directly observe the original lesion and functional areas through the scalp and brain tissue by microscopy. The information thus obtained can be used to form an appropriate flap and establish the optimal surgical trajectory. During lesion resection, the surgeon can visually assess the location and safety of the procedure. The method described in the present report shows the interaction between brain structures and lesion contours by broken and solid lines in the plane of operation. Converting a complex 3D positional relationship into one in the actual plane of operation preserves brain structures. AR technology and microscope-based functional navigation make lesion resection more convenient because the surgeon can use brain structures and lesion contours to discern where and where not to resect.

Utility of iMRI

Brain shift occurs during tumor resection and results in the loss of cerebrospinal fluid, rendering neuronavigation based on preoperative imaging unreliable. Currently, the best way to correct brain shift is by iMRI.[15,16] In this study, we used high-field 1.5T iMRI to correct brain shift, allowing the neurosurgeon to objectively assess the extent of lesion resection so that a decision could be made as to whether the surgery should be continued or terminated. In contrast to initial intraoperative scans, the extent of resection was significantly improved after the final scan. Further resection after scanning did not increase the difficulty of preserving neurologic function but decreased the residual volume from 7.4 ± 10.7 to 3.2 ± 6.4. The timing of MRI for brain shift correction was based on monitoring by the neurosurgeon or the proximity of a boundary. Gliomas are the most common intraxial tumors and are typically not distinguishable from surrounding brain tissue; the combined VR/AR technique is useful for border definition and examining the extent of resection.

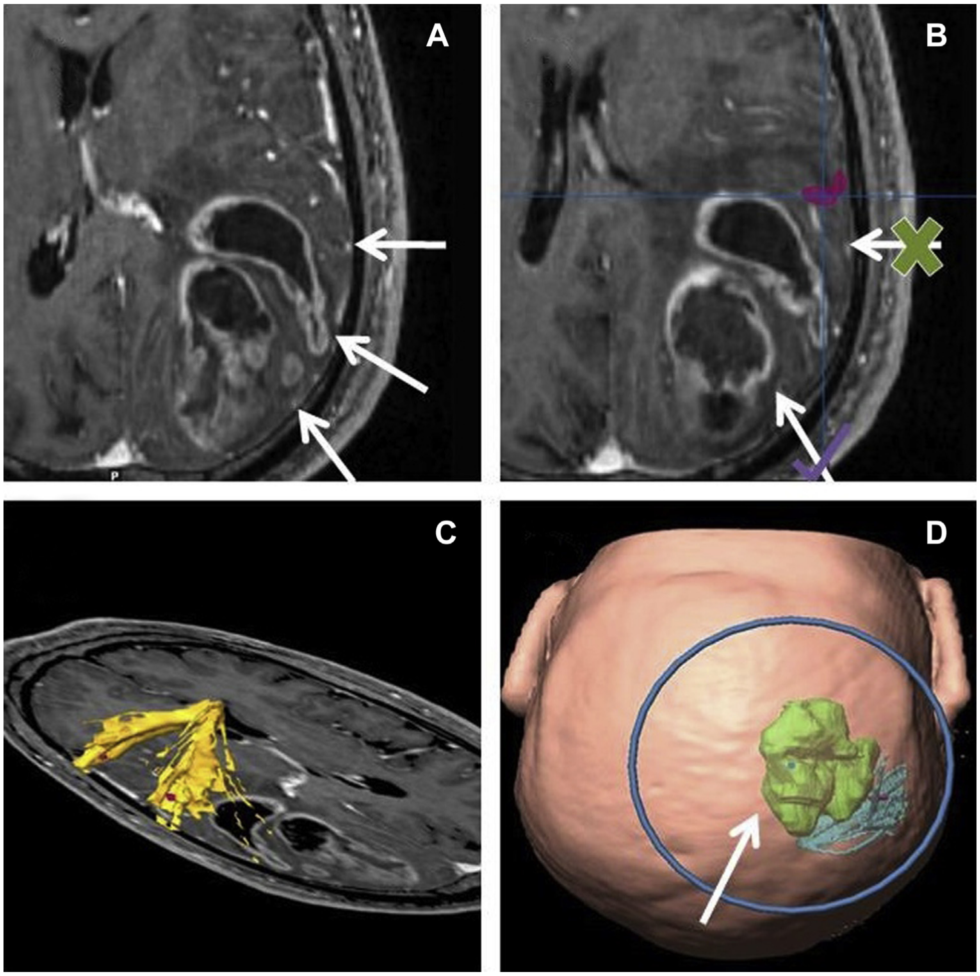

Figure 3. Left temporal-parietal glioma. (**A**) The various ways in which the lesion can be approached are shown by *white arrows*. After integrating the language cortex, the nearest choice was undesirable, whereas the more distant site was safer (**B**); based on this information along with the reconstructed arcuate fasciculus (**C**), the lesion was approached from the rear (**D**).

Table 2. Extent of Tumor Resection Between 2 Groups

	All		HGG		LGG	
	Study Group	Control Group	Study Group	Control Group	Study Group	Control Group
Preoperative volume (cm^3)*	53.1 ± 24.3	49.9 ± 23.8	52.7 ± 27.5	49.5 ± 26.9	53.5 ± 20.8	50.3 ± 21.1
Volume (cm^3) after first intraoperative magnetic resonance image	7.4 ± 10.7	/	8.1 ± 12.7	/	6.7 ± 8.4	/
Final residual volume (cm^3)†	3.2 ± 6.4	8.6 ± 10.5	4.2 ± 8.3	8.2 ± 12.5	2.2 ± 3.4	9.0 ± 8.7
Final extent of resection (%)‡	95.2 ± 8.5	84.9 ± 15.7	95.0 ± 9.9	87.9 ± 15.2	95.5 ± 6.8	82.2 ± 16.0

*Independent samples *t* test, $t = 0.749$, $P = 0.455$ All; $t = 0.463$, $P = 0.645$ for HGG; $t = 0.624$, $P = 0.534$ for LGG.
†Mann-Whitney U test, $Z = -4.066$, $P = 0.000$ All; $Z = -1.727$, $P = 0.084$ for HGG; $Z = -4.489$, $P = 0.000$ for LGG.
‡Mann-Whitney U test, $Z = 4.497$, $P = 0.000$ All; $Z = 2.115$, $P = 0.034$ for HGG; $Z = 4.166$, $P = 0.000$ for LGG.

Table 3. Neurofunction Preservation Rate Between 2 Groups

	Study Group	Control Group	Statistical Analyses and *P* Value
AQ*			
Preoperative	92.1 ± 12.5	91.3 ± 11.1	$t = 0.402$, $P = 0.688$
Postoperative 2 weeks	94.5 ± 10.3	82.9 ± 22.3	$t = 4.051$, $P = 0.000$
Postoperative 3 months	96.0 ± 8.0	89.2 ± 16.5	$t = 3.162$, $P = 0.002$
Muscle strength (mean rank)†			
Preoperative	67.6	67.4	$Z = -0.025$, $P = 0.980$
Postoperative 2 weeks	72.4	60.4	$Z = -2.105$, $P = 0.035$
postop 3 months	74.4	57.7	$Z = -3.116$, $P = 0.002$
Visual field (mean rank)†			
Preoperative	67.9	67	$Z = -0.187$, $P = 0.851$
Postoperative 2 weeks	61.1	76.7	$Z = -2.900$, $P = 0.004$
Postop 3 months	60.6	77.4	$Z = -3.170$, $P = 0.002$

*Independent samples *t* test.
†Mann-Whitney U test.

Comparison of Intraoperative Mapping and Monitoring

Intraoperative mapping and monitoring during awake craniotomy has been used for neurofunctional protection.[17-21] We used this method for eloquent area localization; however, we also performed intraoperative monitoring to confirm the functional area that was localized using fMRI. The 2 methods yielded similar results. Some studies have also described the use of coincident intraoperative monitoring and functional neuronavigation[22-25]; we consider the latter to be convenient and minimally invasive. However, intraoperative mapping and monitoring did not distinguish the tumor border especially for LGG, which could result in the persistence of tumor cells following resection.

VR and AR are seldom applied to neurosurgery. In the present study, we combined the 2 techniques for more precise and accurate neurosurgery. A perfect reproduction of the original in vivo structure can provide more information to the surgeon, thereby simplifying operative planning and execution.

CONCLUSION

The VR and AR technique described in our study can help the neurosurgeon design and optimize surgical planning and intraoperatively visualize structures around the lesions. iMRI can confirm brain shift and provide quality control during the surgical process. Thus, the combination of these techniques can significantly enhance resection of gliomas involving eloquent areas.

ACKNOWLEDGMENTS

The authors thank the members of the Department of Neurosurgery, PLA General Hospital (Hao Tang, MD; Hai-hao Gao, MD; Xing-hua Xu, MD; and Qun Wang, MD) for their collaboration.

REFERENCES

1. Sun GC, Chen XL, Zhao Y, Wang F, Song ZJ, Wang YB, et al. Intraoperative IMRI with integrated functional neuronavigation-guided resection of supratentorial cavernous malformations in eloquent brain areas. *J Clin Neurosci*. 2011;18:1350-1354.
2. Müns A, Mühl C, Haase R, Möckel H, Chalopin C, Meixensberger J, et al. A neurosurgical phantom-based training system with ultrasound simulation. *Acta Neurochir (Wien)*. 2014;156:1237-1243.
3. Chacko AG, Thomas SG, Babu KS, Daniel RT, Chacko G, Prabhu K, et al. Awake craniotomy and electrophysiological mapping for eloquent area tumours. *Clin Neurol Neurosurg*. 2013;115:329-334.
4. Duffau H, Moritz-Gasser S, Gatignol P. Functional outcome after language mapping for insular World Health Organization Grade II gliomas in the dominant hemisphere: experience with 24 patients. *Neurosurg Focus*. 2009;27:E7.
5. Yamaguchi F, Takahashi H, Teramoto A. Intra-operative detection of motor pathways using a simple electrode provides safe brain tumor surgery. *J Clin Neurosci*. 2007;14:1106-1110.
6. Hatiboglu MA, Weinberg JS, Suki D, Tummala S, Rao G, Sawaya R, et al. Utilization of intraoperative motor mapping in glioma surgery with high-field intraoperative magnetic resonance imaging. *Stereotact Funct Neurosurg*. 2010;88:345-352.
7. Mitha AP, Almekhlafi MA, Janjua MJ, Albuquerque FC, McDougall CG. Simulation and augmented reality in endovascular neurosurgery: lessons from aviation. *Neurosurgery*. 2013;72(suppl 1):107-114.
8. Furuya Y, Edwards MS, Alpers CE, Tress BM, Norman D, Ousterhout DK. Computerized tomography of cranial sutures. Part 2: abnormalities of sutures and skull deformity in craniosynostosis. *J Neurosurg*. 1984;61:59-70.
9. Du ZY, Gao X, Zhang XL, Wang ZQ, Tang WJ. Preoperative evaluation of neurovascular relationships for microvascular decompression in the cerebellopontine angle in a VR environment. *J Neurosurg*. 2010;113:479-485.
10. Chen X, Weigel D, Ganslandt O, Buchfelder M, Nimsky C. Prediction of visual field deficits by diffusion tensor imaging in temporal lobe epilepsy surgery. *Neuroimage*. 2009;45:286-297.
11. Furuya Y, Edwards MS, Alpers CE, Tress BM, Ousterhout DK, Norman D. Computerized tomography of cranial sutures. Part 1: comparison

of suture anatomy in children and adults. *J Neurosurg*. 1984;61:53-58.

12. Lu JF, Zhang J, Wu JS, Yao CJ, Zhuang DX, Qiu TM, et al. Awake craniotomy and intraoperative language cortical mapping for eloquent cerebral glioma resection: preliminary clinical practice in 3.0 T intraoperative magnetic resonance imaging integrated surgical suite. *Chinese J Surg*. 2011;49:693-698.

13. Kirkman MA, Ahmed M, Albert AF, Wilson MH, Nandi D, Sevdalis N. The use of simulation in neurosurgical education and training. *J Neurosurg*. 2014;121:228-246.

14. Alaraj A, Charbel FT, Birk D, Tobin M, Luciano C, Banerjee PP, et al. Role of cranial and spinal virtual and augmented reality simulation using immersive touch modules in neurosurgical training. *Neurosurgery*. 2013;72(suppl 1):115-123.

15. Cabrilo I, Sarrafzadeh A, Bijlenga P, Landis BN, Schaller K. Augmented reality-assisted skull base surgery. *Neurochirurgie*. 2014;60:304-306.

16. Leuthardt EC, Lim CC, Shah MN, Evans JA, Rich KM, Dacey RG, et al. Use of movable high-field-strength intraoperative magnetic resonance imaging with awake craniotomies for resection of gliomas: preliminary experience. *Neurosurgery*. 2011;69:194-205.

17. Mahvash M, Besharati Tabrizi L. A novel augmented reality system of image projection for image-guided neurosurgery. *Acta Neurochir (Wien)*. 2013;155:943-947.

18. Sun GC, Chen XL, Zhao Y, Wang F, Hou BK, Wang YB, et al. Intraoperative high-field magnetic resonance imaging combined with fiber tract neuronavigation-guided resection of cerebral lesions involving optic radiation. *Neurosurgery*. 2011; 69:1070-1084.

19. Kuhnt D, Bauer MH, Nimsky C. Brain shift compensation and neurosurgical image fusion using iMRI: current status and future challenges. *Crit Rev Biomed Eng*. 2012;40:175-185.

20. Sanai N, Mirzadeh Z, Berger MS. Functional outcome after language mapping for glioma resection. *N Engl J Med*. 2008;358:18-27.

21. Maesawa S, Fujii M, Nakahara N, Watanabe T, Wakabayashi T, Yoshida J. Intraoperative tractography and motor evoked potential (MEP) monitoring in surgery for gliomas around the corticospinal tract. *World Neurosurg*. 2010;74: 153-161.

22. Ferroli P, Tringali G, Acerbi F, Schiariti M, Broggi M, Aquino D, et al. Advanced 3-dimensional planning in neurosurgery. *Neurosurgery*. 2013;72(suppl 1):54-62.

23. Cabrilo I, Bijlenga P, Schaller K. Augmented reality in the surgery of cerebral arteriovenous malformations: technique assessment and considerations. *Acta Neurochir (Wien)*. 2014;156: 1769-1774.

24. Trantakis C, Tittgemeyer M, Schneider JP, Lindner D, Winkler D, Strauss G, et al. Investigation of time-dependency of intracranial brain shift and its relation to the extent of tumor removal using intra-operative MRI. *Neurol Res*. 2003;25:9-12.

25. Zhu FP, Wu JS, Song YY, Yao CJ, Zhuang DX, Xu G, et al. Clinical application of motor pathway mapping using diffusion tensor imaging tractography and intraoperative direct subcortical stimulation in cerebral glioma surgery: a prospective cohort study. *Neurosurgery*. 2012;71:1170-1183.

Conflict of interest statement: The authors have no personal financial or institutional interest in any of the drugs, materials, or devices described in this article. This study was funded by grants from the Science and Technology Projects of Hainan province (2015SF16); Technological Innovation Foundation of the PLA General Hospital (14KMM37); Medical and Technical Innovation Project, Sanya, Hainan Province (2014YW31); Health Industry Research Project of Hainan Province (14A210218); Natural Science Foundation of Hainan Province (20168362); National Natural Science Foundation of China (81271515); and the Key Research and Development Project of Hainan Province (ZDYF2016118). The sponsors had no role in the design or conduct of this research.

Received 1 May 2016; accepted 30 July 2016

Citation: World Neurosurg. (2016) 96:375-382.
http://dx.doi.org/10.1016/j.wneu.2016.07.107

Journal homepage: ***www.WORLDNEUROSURGERY.org***

Available online: ***www.sciencedirect.com***